Cross-linked and hydrophobized hyaluronic acid-based controlled drug release systems

Edit Csapó[a,b,*], Hajnalka Szokolai[b], Ádám Juhász[a,b], Norbert Varga[b], László Janovák[b], Imre Dékány[a,b]

[a] MTA-SZTE Biomimetic Systems Research Group, Department of Medical Chemistry, Faculty of Medicine, University of Szeged, H-6720 Dóm square 8, Szeged, Hungary

[b] Department of Physical Chemistry and Materials Science, University of Szeged, H-6720, Aradi v.t.1, Szeged, Hungary

[*]Corresponding author: E. Csapó, *email*: juhaszne.csapo.edit@med.u-szeged.hu

Abstract

This work demonstrates the preparation, structural characterization, and the kinetics of the drug release of hyaluronic acid (HyA)-based colloidal drug delivery systems which contain hydrophobic ketoprofen (KP) as model molecule. Because of the highly hydrophilic character of HyA the cross-linked derivatives at different cross-linking ratio have been synthesized. The hydrophobized variants of HyA have also been produced by modifying the polymer chains with cetyltrimethylammonium bromide (CTAB) at various HyA/CTAB ratios. Due to modifications the coherent structure of HyA changes into an incoherent colloidal system that were verified by rheological investigations. Nearly 70% of the encapsulated KP dissolve from the totally cross-linked HyA carrier but the release rate of KP is about 20% (after 8h) from the CTAB-modified colloidal system at HyA monomer/CTAB 1:0.8 mass ratio. It has been verified that the modified HyA may be a potential candidate for controlled drug release of hydrophobic KP molecules.

Keywords: hyaluronic acid, cross-linking, hydrophobization, nanocarrier, rheology, controlled drug release

1. Introduction

All areas encapsulating nano- or microparticle-based drug delivery systems have become some of the most fascinating research areas in modern pharmaceutical development. Several biodegradable macromolecules such as polyesters, proteins, polysaccharides, polyelectrolytes, lipids *etc*. (Benkő et al., 2015; Csapó et al., 2016; Danhier et al., 2012; Kumari et al., 2010; Padilla et al., 2002; Palumbo et al., 2006; Pasqui et al., 2012), or inorganic materials (layer double hydroxides (LDH), clays, mesoporous silica *etc*. (Deák et al., 2018; Varga, Benko, Sebok, Bohus, et al., 2014) are used as drug carriers in order to achieve a targeted drug delivery system and also a controlled drug release process. Generally, albumin proteins, biocompatible polymers, liposomes, or solid lipid NPs have been utilized for encapsulation of non-steroidal anti-inflammatory drugs (NSAID) such as ibuprofen, meloxicam *etc*. (Benkő et al., 2015; Csapó et al., 2016; Varga et al., 2014). Ketoprofen (KP) also belongs to NSAID and is widely used to treat postoperative pain, including patients after a gastric resection.

Hyaluronic acid (HyA) is a well-known linear polysaccharide of alternating units of β-1,4-*D*-glucuronic acid and β-1,3-*N*-acetyl-*D*-glucosamine. (Berkó et al., 2013; Bodnár et al., 2009; Hashad et al., 2017; Lee et al., 2015; Maroda et al., 2011; Wang et al., 2017) Because of the biocompatible, biodegradable, non-toxic, non-immunogenic and non-inflammatory features this biomaterial is an ideal candidate for several medical and pharmaceutical applications. At physiological conditions (pH, ionic strength) the HyA molecules have a negative charge (hyaluronate form) which results in an extremely high hydrophilic property. Thanks to the hydrophilic character of HyA it is present in several biological fluids, the highest amount can be found in the extracellular matrix of the soft connective tissues. The main disadvantage of this hydrophilic character is that HyA molecules, without chemical structural modification, cannot be simply used as a carrier. In most cases chemical preparation routes have been selected in order to synthesize the hydrophobized derivatives of HyA (*e.g.* biocompatible polymer (HyA/polylactic acid (Mayol et al., 2014)) or different alkyl- and aryl-functionalized derivatives (HyA/decylamine(DA)) (Lee et al., 2015; Vafaei et al., 2016). Some cases the HyA has been used as surface functionalizing agent for preparation of *e.g.* core-shell type NPs (HyA/Human serum albumin-covered chitosan NPs) via electrostatic adsorption of the negatively charged HyA onto the surface of core NPs which has a positive surface charge (Hashad et al., 2017). Besides these derivatives the cross-linked variants of HyA can also be used to encapsulate different drugs (Berkó et al., 2013; Bodnár et al., 2009;

Maroda et al., 2011). Various techniques have been developed for the production of cross-linked HyA, but one of the commonly used method is the carbodiimde technique. (Bodnár et al., 2009; Maroda et al., 2011) During this procedure the covalent cross-linking of the carboxyl functional groups of HyA molecules is carried out with a diamine in an aqueous medium at room temperature. The main advantage of this technique is that stable colloidal particles can be formed in water without the use of any surfactant or other organic solvent. Another possibility is the chemical modification of the HyA molecules by linking aliphatic or aromatic functional groups to the previously mentioned carboxyl moiety which gives the HyA macromolecules hydrophobicity.(Choi et al., 2009) Moreover, the less-known neutralization of HyA via the formation of electrostatic interactions using positively charged amines containing long aliphatic chains like cetyltrimethylammonium bromide (CTAB) also results in HyA particles having hydrophobic nature. (Kargerová et al., 2014; Oueslati et al., 2014; Sauerová et al., 2015) In previous work by other research groups, the KP was encapsulated in different polymers (*e.g.* poly (D, L-lactic acid) (PDLLA) or Eudragit) or alginate and gelatin-based carriers but the HyA has not been used before for the direct encapsulation of KP molecules. (Arida & Al-Tabakha, 2007; Del Gaudio, Russo, Rosaria Lauro, Colombo, & Aquino, 2009; Vučen et al., 2013)

In this work hydrophobic KP, as the model drug molecule, has been used to develop and characterize different types of modified HyA-based systems for controlled drug release. The cross-linking of HyA has been carried out in aqueous media at different ratios of cross-linking (50; 75 and 100%). Moreover, the hydrophobized derivatives of HyA have also been prepared by using CTAB at three different HyA monomer/CTAB mass ratios (1:0.2; 1:0.5; 1:0.8). Besides structural characterizations the drug release process has also been investigated and the experimental results of different colloidal systems were interpreted. One of the main motivation of this work was to introduce that the extreme hydrophilic HyA after structural modifications is applicable for encapsulation of highly hydrophobic KP small molecules which results in the formation of an effective HyA-based nanosized colloidal systems and a controlled KP release is also feasible.

2. Materials and Methods

2.1 Materials

Hyaluronic acid sodium salt (HyA, 200-500 kDa) was obtained from Gedeon Richter Plc. Ketoprofen (KP; $C_{16}H_{14}O_3$; ≥98%) and CTAB ($CH_3(CH_2)_{15}N(Br)(CH_3)_3$; 95%), sodium phosphate dibasic dodecahydrate ($Na_2HPO_4 \times 12H_2O$; 98.5%) and sodium phosphate

monobasic monohydrate ($NaH_2PO_4 \times H_2O$; ≥99%) were purchased from Sigma-Aldrich. Sodium chloride (NaCl; a.r.), from Molar Chemicals, was used to prepare isotonic (150 mM) NaCl solution. For the cross-linking reaction 2,2'(ethylenedioxy)bis(ethylamine) (EDEA; $NH_2CH_2CH_2OCH_2CH_2OCH_2CH_2NH_2$; 98%) and 1-[3-(dimethylamino)propyl]-3-ethylcarbodiimid methiodide (EDC methiodide; $C_2H_5N{=}C{=}N(CH_2)_3N(CH_3)_3I$) were obtained from Sigma-Aldrich. Highly purified water was obtained by deionization and filtration with a Millipore purification apparatus (18.2 MΩ·cm at 25 ºC). All solvents and reagents used were of analytical grade and no further purification were made.

2.2 Experimental procedures of the HyA modifications

Cross-linked (cl) HyA derivatives were prepared according to the previously published procedure reported by Bodnár *et al.*(Bodnár et al., 2009) The synthesis was performed at room temperature. Namely, 200 mg HyA was dissolved in water to produce 1 mg/mL solution then the pH was adjusted to pH = 5.5. The stoichiometric ratio of cross-linking was 50%, 75% and 100% resulting in cl-HyA/50%, cl-HyA/75% and cl-HyA/100% samples. Accordingly, 1.88 mL, 2.82 mL and 3.76 mL EDEA solution (1 v/v%, pH = 5.5) was added to the HyA solution and mixed for 30 min. Then 80 mg, 120 mg and 160 mg EDC methiodide was dissolved in water and added to the mixture drop by drop, respectively. After an overnight stirring the product was purified by dialysis for 7 days against distilled water and the aqueous solution of the final product was freeze-dried. For CTAB modification different calculated amount of surfactant was added to the aqueous solution of HyA to change the hydrophobicity. The mixture was stirred for 30 min before further use.

2.3 Preparation of KP-containing systems

Because of the low solubility of KP in pure Milli-Q water (c_{max} = 0.051 mg/mL) all drug containing samples were prepared in phosphate buffer solution (PBS) at pH = 7.4 at 25 °C using constant ionic strength (0.9 % NaCl) which highly increased in the KP solubility (c_{KP} = 20 mg/mL). In all cases constant KP (c_{KP} = 20 mg/mL) and constant HyA concentrations (100.0-100.0 mg lyophilized HyA and cl-HyA/mL) were used. The aqueous KP solutions were added to the different individual cl-HyA and HyA/CTAB samples which resulted in the formation of a gel-like structure after 24 h. After KP loading the samples were diluted to 0.1% and centrifuged (8000 rpm, 10 min). The supernatant contained only 4.5-5.0 % remained KP molecules determined by the previously registered spectrophotometric calibration curve. According to this determination method the loading efficiency is *ca.* 95.5-95.0%.

2.4 Methods for structural characterizations

High-resolution transmission electron microscopy (HRTEM) images were recorded on a Tecnai G2 instrument at 200kV accelerating voltage and they were analyzed using ImageJ software. The particle size and zeta potential values were determined by dynamic light scatteing (DLS) with a Zetasizer Nano ZS ZEN 4003 apparatus (Malvern Ins., UK) equipped with a He-Ne laser (λ = 633 nm). The measurements were performed at 25 ± 0.1 °C, with an angle detection of 173° in a clear disposable zeta cell. In order to determine the maximum amount of CTAB to be added prior to precipitation 0.02 M of CTAB was added stepwise (20-20 µL/ step) to 0.2 mg/mL concentration of HyA in PBS and the zeta potential values were registered with DLS. Turbidity measurements were performed by a Precision Bench Turbidity Meter LP2000 (Hanna Ins.), while the conductivity was measured by a Radelkis OK- 114 conductometer equipped with an electrode with sheet plates. The Fourier transform infrared (FT-IR) spectroscopy studies were performed by using Jasco FT/IR-4700 spectrometer with ATR PRO ONE Single-reflection accessory (ABL&JASCO, Hungary). Spectra were registered at 4 cm^{-1} optical resolution by averaging 256 interferrograms.

2.5 Isothermal Titration Calorimetry (ITC) studies

Thermometric titration experiments were performed at 298.15 K with a computer-controlled VP-ITC power-compensation microcalorimeter (MicroCal) in order to determine the degree of the charge compensation of the CTAB in presence of HyA. Deionized water or HyA solution (1.4 mL) in the sample cell was titrated under constant stirring with 300 µL of CTAB solution in aliquots of 10 µL in periodic time intervals of 5 min. The enthalpograms (calorimeter power signal vs time) were evaluated by means of Origin Microcal 7.1. software. ITC curves were successfully fitted by using the sigmoidal Boltzmann equation. The modified version of Boltzmann equation has been used to improve the precision of the determination of the critical micellization concentration (*cmc).*(Juhász et al., 2017; Kiraly et al., 2001)

2.6 Rheological studies

All rheological measurements were performed using an Anton Paar Physica MCR 301 Rheometer (Anton Paar, GmbH, Germany) at 25.0±0.1 °C to provide concentration-dependent structural information on the modified HyA-based drug carrier systems. The measuring system equipped with a 25 mm diameter parallel cone-plate geometry (CP25-1-SN12204), a double-gap- (DG26.7-SN12740) and a concentric cylinder geometry (CC27-SN12793). The rheometer utilized a temperature controlled water bath in combination with a

Peltier heating system for accurate control. Detailed parameters of the rheological measurements, as well as the evaluation process, are summarized in the Supplementary.

2.7 In vitro drug release experiments

The release rate of KP molecules was determined by spectrophotometric measurements detected the characteristic absorbance band of KP at 260 nm using a UV-1800 (Shimadzu) double beam spectrophotometer with a 1 cm quartz cuvette in the range of 200-500 nm. The *in vitro* drug release experiments were carried out in a phosphate buffer (PBS, pH = 7.4) at 25 °C. A cellulose membrane (Sigma-Aldrich) was used as a dialysis membrane. The release process was followed for 480 min (8 h). Samples were taken every 10 minutes in the first hour and then once per hour. Analysis of in vitro drug release data helps evaluate the release kinetics and mechanism. Numerous mathematical models (zero-order, first-order, Weibull, Hixone-Crowell, Korsmeyere-Peppas, *etc*.) have been used to describe the release properties of the drug molecules (Costa et al., 2001; Peppas et al., 1977). The detailed description of the different kinetic models is summarized in Supplemetary. To determine the value of the kinetic constants and other parameters of the applied release kinetic models, the sum of the square of differences between the measured and predicted concentration values have been minimalized using a spreadsheet based computer application for nonlinear parameter estimation (Juhász et al., 2016; Juhász, Csapó, Vécsei, & Dékány, 2017).

3. Results and Discussion

3.1 Structural characterization of the different HyA-based carriers

Due to its highly hydrophilic nature, HyA as a possible carrier for encapsulation of hydrophobic agents requires structural modifications. Both the cross-linked (cross-linking ratio of 50, 75 and 100%) and hydrophobized derivatives (partly neutralization with positively-charged amines) of the HyA carrier have been successfully prepared. FT-IR studies, which are in good agreement with the previously published data, (Barbucci et al., 2002; Jiang et al., 2015) have been performed to identify the success of the formation of cross-linking, the results are presented in Fig.S1.

The different HyA modifiation methods are summarized in **Scheme 1**.

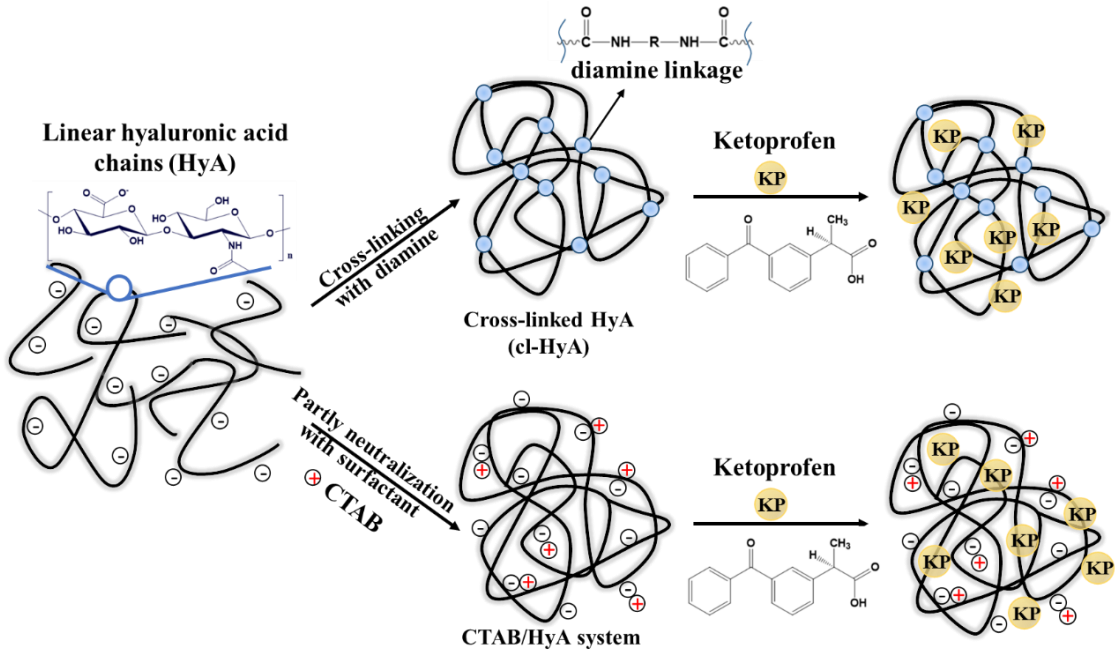

Scheme 1. Schematic representation of HyA modifications: cross-linking and neutralization with positively-charged amine.

Due to structural modifications it was found that increasing cross-linking ratio from 50 % to 100% results in the formation of nanosized particles, with an increasing size of *ca*. 45 nm (cl-HyA/50%) and *ca*. 110 nm (cl-HyA/100%). **Figure 1.** shows the particle size distributions of cl-HyA carrier systems determined by DLS with a representative TEM image of the cl-HyA/100% particles. The registered TEM image is in accord with the DLS results, the slight difference between the results can be explained by the hydrodynamic diameter. However the particle size increases with the cross-linking ratio, the presence of more polydispersed systems can be confirmed by DLS. In contrast, the measured Zeta-potential values at neutral pH (pH ~ 7.0) shows an increased stability (cl-HyA/50%: ζ = -13.8 ± 0.1 mV, cl-HyA/75%: ζ = -20.0 ± 2.1 mV, cl-HyA/100%: ζ = -23.6 ± 0.6 mV) for the application of higher concentration of cross-linker. For HyA/CTAB systems the structure, the charge, as well as the optimal ratio of HyA and CTAB, were determined by conductometric, turbidity, Zeta-potential and ITC measurements in an aqueous solution at 25 °C. It is well known that the CTAB molecules are capable of forming micelles when the concentration reaches the *cmc*.

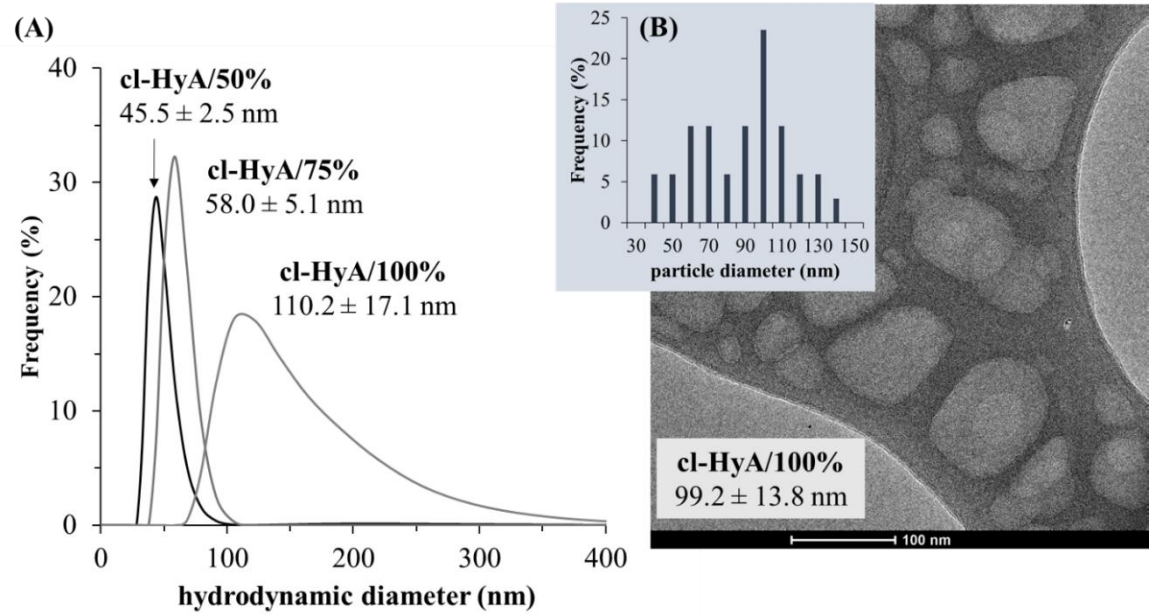

Figure 1. Particle size distribution of the different cl-HyA carriers determined by DLS (A) and a representative HRTEM image and particle size distribution of the cl-HyA/100% system (B).

According to the parallel conductometric measurements 0.94 ± 0.01 mM of *cmc* value is obtained for CTAB (**Figure 2A**), while same 0.94 ± 0.01 mM value was determined by ITC as the grey continuous line represents on **Fig. 3.B**.

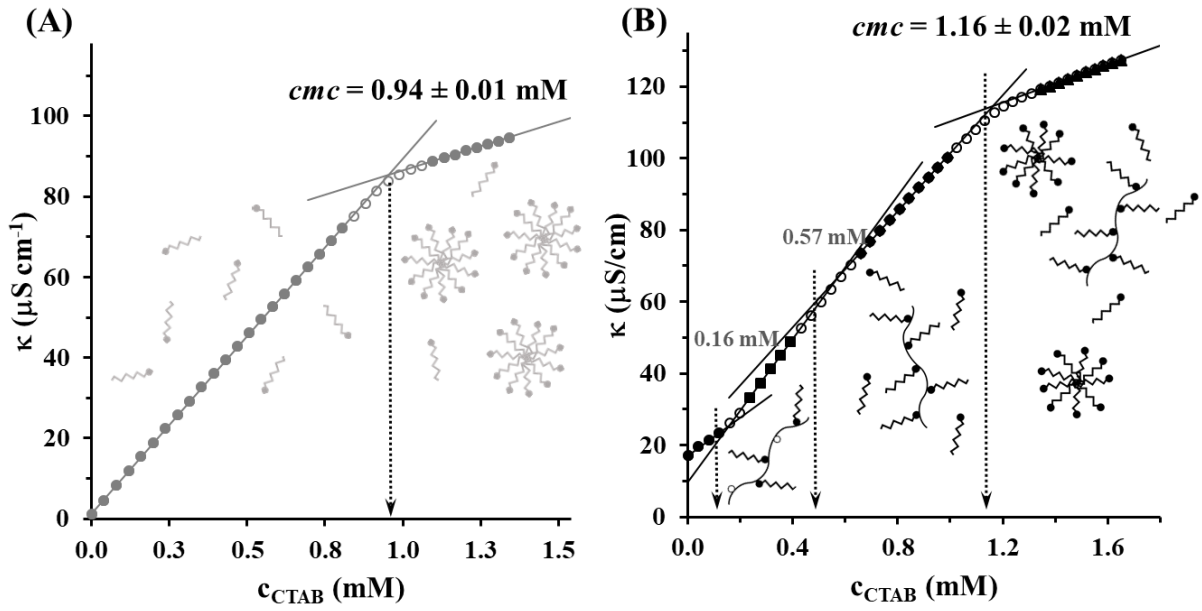

Figure 2. Determination of the *cmc* of CTAB by conductometric measurements in the absence (A) and in the presence (B) of HyA (c_{HyA}= 0.1 mg/mL).

Both the conductometric and ITC studies have been carried out in the presence of 0.1 mg/mL of HyA and as **Figure 2B and Figure 3B** represent, the *cmc* value shifted to 1.16 ± 0.02 mM, respectively.

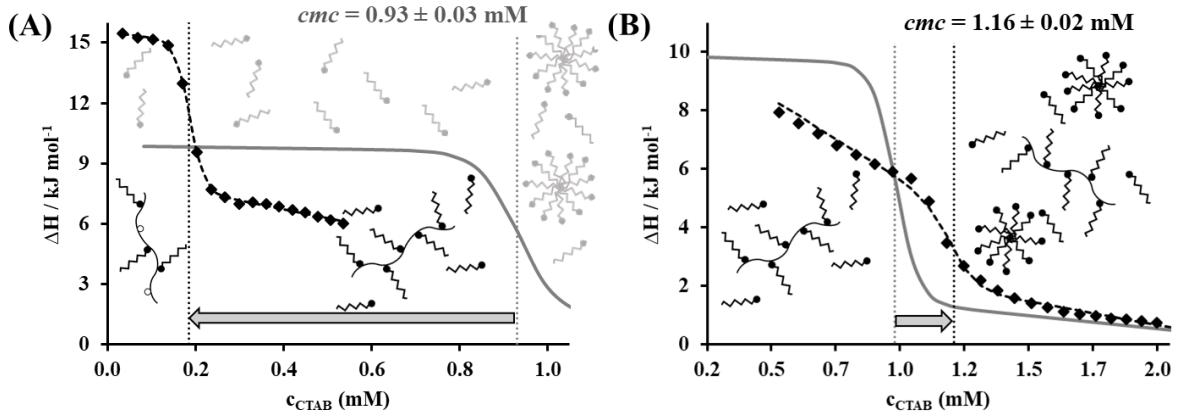

Figure 3. Calorimetric enthalpies of dilution obtained from ITC experiments for CTAB in the presence of HyA (c_{HyA} = 0.1 mg/mL) at c_{CTAB} = 12 mM (A) and c_{CTAB} = 5 mM (B) at 298 K.

The continuous grey lines in **Fig. 3** represent the enthalpogram of pure CTAB in the absence of HyA under the same conditions. The degree of this shift (presence of excess CTAB) strongly depends on the total amount of HyA in the sample. Calculating with the HyA concentration we can conclude that the negatively charged HyA, before the formation of micelles, is totally neutralized by CTAB. At the neutralization point the CTAB/HyA monomer ratio is *ca*. 1:1 molar (0.96:1.0 mass ratio) obtained by conductometry and ITC studies. In order to determine the equivalent charge of the linear HyA, an additional ITC measurement was performed with diluted surfactant solution (c_{CTAB} = 5 mM, c_{HyA} = 0.1 mg/mL). As can be seen in **Figure 3A** an inflection point is observed at 0.2 ± 0.01 mM which corresponds to nearly 1.2:1.0 surfactant/HyA monomer molar ratio. This observation also supports the equivalent charge compensation of HyA monomer with CTAB. As **Fig. 4** shows the Zeta potential of the negatively-charged polymer reaches the zero value at 0.95:1.0 CTAB/HyA monomer mass ratio which is in accord with the conductometry, and ITC experiments. Both the turbidity measurements and the change of the average particle diameter of the CTAB/HyA system confirm the aggregation of the polymer chains after the charge compensation of the carboxyl groups of HyA.

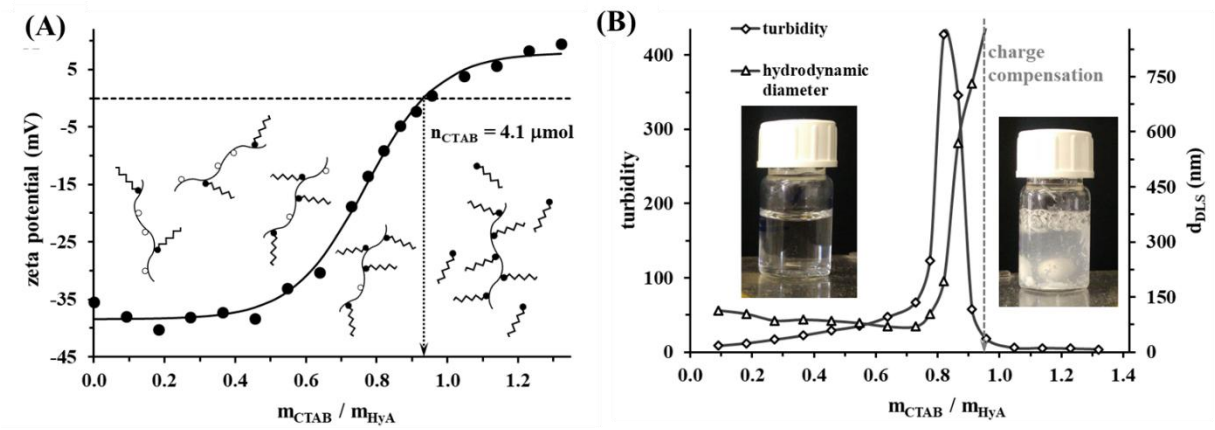

Figure 4. Zeta potential (A), turbidity and hydrodynamic diameter (B) of the HyA/CTAB system as a function of increasing CTAB/HyA monomer mass ratio (c_{HyA} = 0.2 mg/mL) The (B) represents the photos of the samples before (at m_{CTAB}/m_{HyA}=0.2) and after (at m_{CTAB}/m_{HyA}=0.95) charge compensation of HyA.

Above this surfactant concentration (0.95 mg CTAB/1.0 mg HyA monomer) the particle size rises dramatically (from 50 nm to *ca*. 750 nm) while the turbidity decreases due to the aggregation of the hydrophobized and neutralized polymer chains. The registered DLS curves of HyA/CTAB system at different m_{HyA}/m_{CTAB} ratios are presented in Fig. S2.

3.2 Concentration-dependent rheological characterization of the aqueous HyA solutions and hydrogels before structural modifications

Based on the rheological studies we found that, the increase in polymer concentration resulted in a dramatic change in the rheological behavior. The HyA solutions show Newtonian, non-Newtonian and viscoelastic behavior as the concentration increases from 0.05 to 100 mg/mL. The viscosities of diluted and moderately concentrated polymer solutions were determined by a rotational technique based on the fitting of registered flow curves. In the case of much dilute solutions, the linear flow curves prove the validity of the Newton law (**Figure S3**). For these extremely diluted polymer solutions, which are usually considered as a molecular solution, the viscosity variations are associated with a behavior (deformation, orientation etc.) of separate molecules under flow conditions. Generally, the viscosities of moderately concentrated solutions of high-molecular weight polymers are known to be variable quantities which decrease with increasing shear rate. This shear-thinning effect has been understood for a long time and as Fig. S4 shows similar behavior was observed for HyA above 1.00 mg/mL concentration. In the case of these concentrated solutions, a varying viscosity is assumed to be due to the entanglement of linear polymer chains. An alternative explanation of this effect, is

based on an assumption of weak macromolecular cross-linking. These secondary bindings disappear and reappear again as a result of thermal motion, and the average number of these weak cross-links in the shear flow decreases when the shear rate is increased. While this characteristic is very desirable, it creates problems when attempting to measure the viscosity of HyA solutions and concentrated gels. A single-point viscosity test such as that typically conducted on a simple viscometer is insufficient to fully characterize the material. Instead of this, a viscosity/shear rate profile (such as that shown in **Figure S4**) is more suitable as a means of measuring this material. Moreover, we report the results of the dynamic measurements, which show the change of the loss and the storage modulus (*G'* and *G''*) as a function of amplitude, under 10 s^{-1} oscillation frequency . All the samples were tested but only some results are presented for clarity. For the linear polymer (**Figure 5**), we observe the expected behavior. Polymer gels essentially show elastic character at low strain, while at high strain the loss modulus dominates (*G'' > G'*). The distance between the *G'*, and *G''* curves has no such relevance as the ratio *G''*/*G'* which is equal to tanδ, this parameter is a measure of the internal friction of the material in that condition.

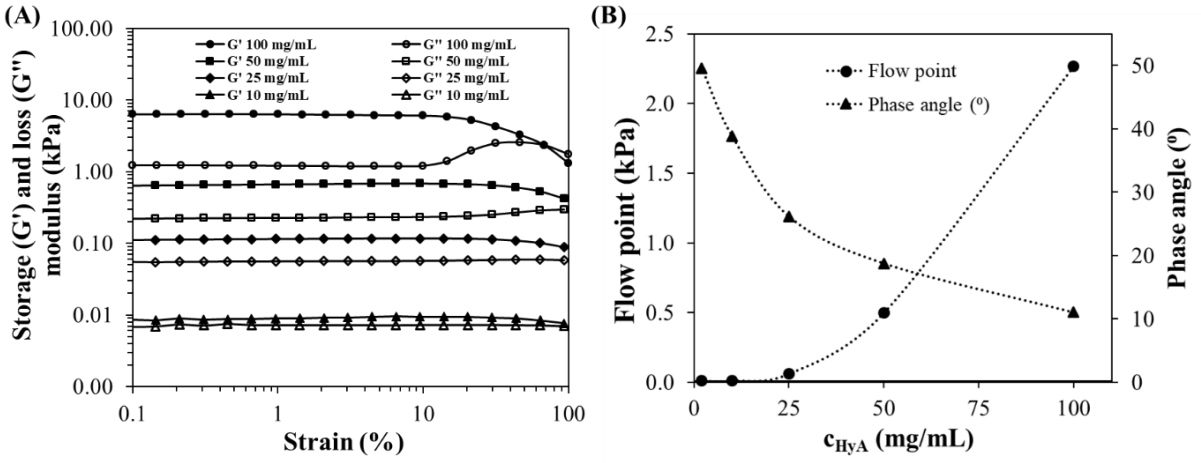

Figure 5. Strain (A) and concentration (B) dependence of the viscoelastic parameters (storage modulus (solid symbols) and loss modulus (hollow symbols), flow point and phase angle) of linear HyA hydrogels.

When *G''* is higher than G', tanδ is the larger one we can say that the sample is more viscous than elastic, and when G' is higher and tanδ is the smaller one the sample shows an elastic property. Amplitude scans of the solvated linear HyA shows that the *G''*/*G'* ratio does not change as strain increases from 0.1 to 10.0%, it means that the internal friction is independent of strain in this region. Above strain value of 10%, the samples show non-linear dependence,

according to the pseudo-plastic or plastic behavior. The point where *G''* crosses G' is denoted as the flow point, and above this strain value the viscous behavior dominates. **Figure 5.B** clearly shows that the flow points increase dramatically, while the phase angle decreases as the polymer concentration increases. The decrease of the phase angle indicates the change from Newtonian behavior to elastic behavior, which confirms viscoelastic fingerprint characterizing concentrated HyA solutions with weak gel-like behavior (Iannitti et al., 2013; Liang et al., 2007).

3.3. Rheological characterization of the hydrophobized CTAB/HyA systems

To characterize the hydrophobized form of the polymer, a constant (0.1 mg/mL) initial HyA concentration was chosen for the steady shear rate measurements of the CTAB solution diluted HyA samples and a larger concentration (50 mg/mL) was applied in the case of amplitude sweep investigations. As can be seen in **Figure 6.** the apparent viscosity of the polymer solution continuously decreases, due to the added surfactant, and a breakpoint can be observed on the viscosity vs. molar ratio (n_{CTAB} /$n_{monomer}$) curve. After extraction the dilution effect only in the pre-break region can be observed. Above *ca*. 1:1 surfactant/monomer molar ratio, the viscosity of the neutralized and thus the hydrophobized polymer solution, shows a rising trend. After this observation it can be stated that in addition to conductivity and ITC measurement a modified rheological investigation also suitable for detection of the structural change of the polymer – surfactant colloid system.

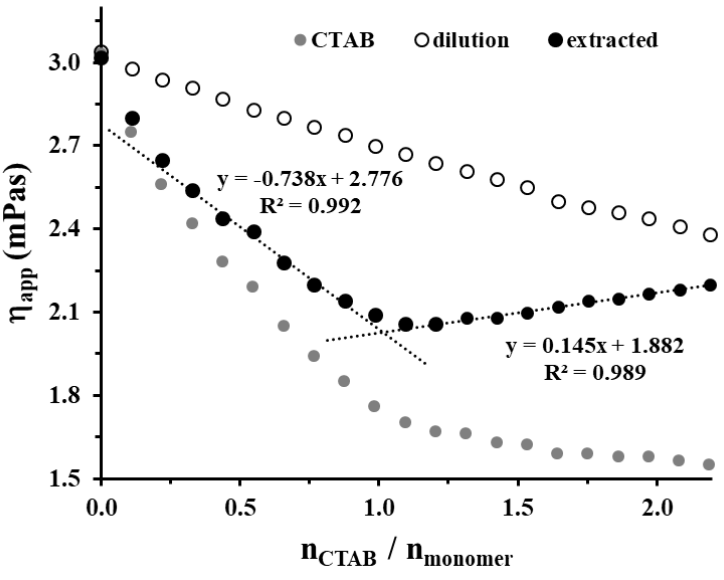

Figure 6. Steady shear rate determined apparent viscosity of linear HyA (c_{HyA} = 0.1 mg/mL) titrated with CTAB (c_{CTAB}= 25.0 mM) solution.

As illustrated in **Figure 7.** the varying degrees of hydrophobized polymer based hydrogels, show elasticity at low strain, while at high strain range the loss modulus dominates (*G'' > G'*) as the above reported linear HyA hydrogels. As a result of added surfactant at 10 mg/mL CTAB concentration (20% of the neutralization needed surfactant amount) the flow point increased dramatically and it is slightly reduced by the effect of the following (50% and 80%) additional surfactant. The opposite tendency can be observed with regard to the change of phase angle value in the function of CTAB concentration. When the concentration of polymer is over the 50 mg/mL and surfactant is 10.0 mg/mL or lower the hydrogel becomes more elastic than without surfactant while above this surfactant amount the elastic behavior turns Newtonian. The same trend was observed in the case of varying degrees of cross-linked polymer hydrogels (**Figure S5.**) where the flow point almost reaches the zero value due to the structure modification of polymer chains, and the changes of phase angle showed a more and more viscous character. The latter outlined two observations confirm the assumption that both the added CTAB, and the cross-linking agent break the spontaneously formed coherent structure from the solvated biopolymer.

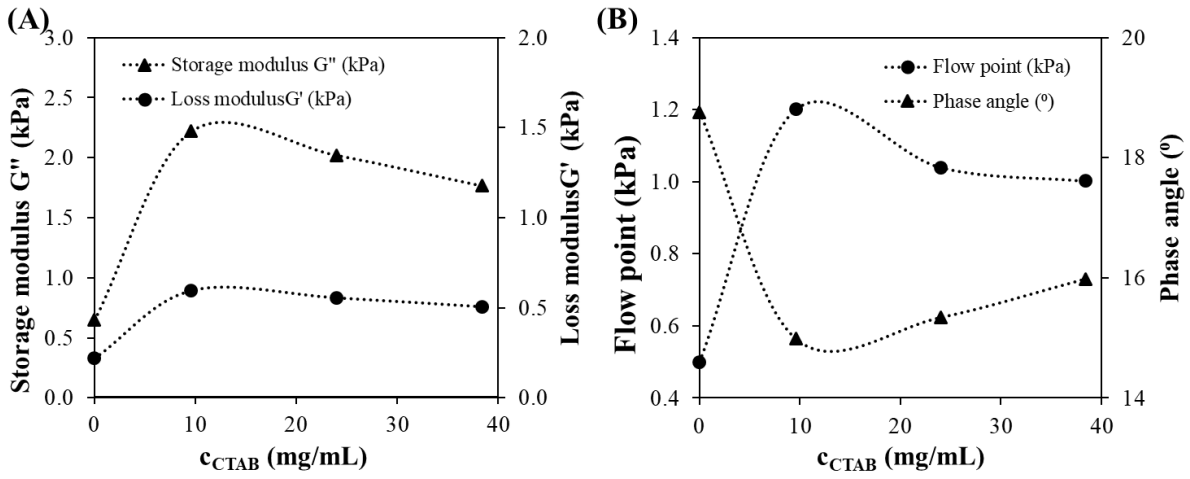

Figure 7. Amplitude sweep determined rheological parameters (A: storage modulus and loss modulus; B: flow point and phase angle) of linear HyA hydrogels (c_{HyA} = 50 mg/ mL) as a function of c_{CTAB}.

3.4 *In vitro* drug release experiments

The detailed rheological characterization of the pure and modified drug carrier systems greatly contributes to the better understanding the mechanism of the drug release process. The mechanism of drug release from the HyA-based carriers was investigated using model-dependent methods. The drug release results were fitted into first-order kinetics, Korsmeyer–

Peppas and Weibull models. Drug release curves of KP from varying degrees of hydrophobized or cross-linked polymer-based carriers are depicted in **Figure 8**. As it can be seen, all the formulations are able to impede KP release for more than 6 h, but the release of the drug from the cross-linked polymer is almost complete within 7 h. In particular, the release kinetic of KP from cl-HyA/50% is the fastest and, above all, poorly controlled. By adding the linker from 50% to 75 and 100% into the polymer it was possible to achieve a more accurate control over drug release from the polymeric carrier. However, it should be noted that nearly 80% is released from the total drug content in the case of cl-HyA/100% at the end of the seventh hour (**Figure 8A**). On the other hand, using the least amount of surfactant (**Figure 8B**) caused only 60% of the active ingredient to dissolve during the experiment.

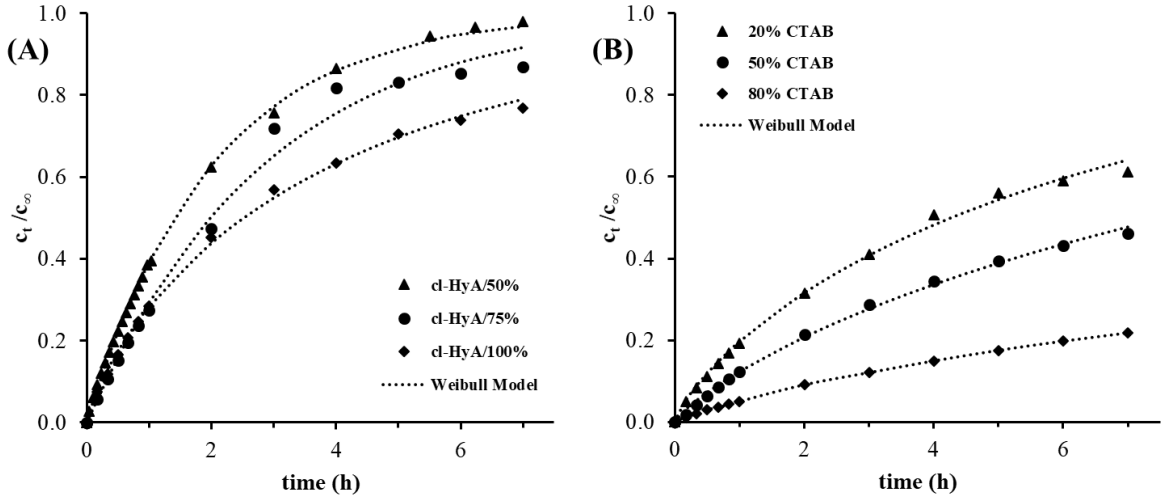

Figure 8. Release profiles and Weibull kinetic model-predicted release curves of KP from varying degrees cl-HyA-based (A) and CTAB hydrophobized (B) drug carriers.

Keeping regard the values of coefficient of determination, (R^2) from **Table 1**, the Weibull model was the best and the Korsmeyer and Peppas model was the second best model for the hydrophobized polymer. While in the case of cl-polymers the Weibull model was the best, and first order model is the second best model for describing the release profiles. Although the fitting of the Korsmeyer and Peppas equation does not produce a good description of dissolution profile as well as the Weibull model, the values of the matching parameters (k_m and n) also carry important information. Hydrophobized HyA exhibited a release exponent n, values of 0.60; 0.70 and 0.75, indicating that the drug release from surfactant – polymer

system might have followed both drug diffusion and the erosion of matrix in an anomalous non-Fickian manner.

Table 1. Fitting results of the experimental KP release data to different kinetic equations, for several formulations

Formulation	First-order		Korsmeyer–Peppas			Weibull		
	k (h^{-1})	R^2	k_m (h^{-n})	n	R^2	a	b	R^2
20% CTAB	0.16	0.9881	524	0.6039	0.9819	0.0003	0.7935	0.9971
50% CTAB	0.10	0.9892	149	0.6975	0.9941	0.0002	0.8210	0.9978
80% CTAB	0.04	0.9907	41	0.7484	0.9989	0.0001	0.7950	0.9995
cl-HyA/50%	0.50	0.9995	1401	0.5539	0.9799	0.0001	0.9913	0.9995
cl-HyA/75%	0.34	0.9977	698	0.6127	0.9783	0.0001	1.0095	0.9977
cl-HyA/100%	0.26	0.9901	1126	0.5497	0.9886	0.0005	0.7950	0.9986

Release exponents of the cross-linked carriers are much closer to the limit (n = 0.45) which indicates the diffusion-controlled Fickian drug release. In addition, the fact that the value of the release exponent of the hydrophobized matrix continually decreases as the amount of surfactant increases, shows that the contribution of anomalous diffusion is gets stronger. Based on the observation of previous parts (change of the zeta potential, turbidity and particle size values as a function CTAB amount), it can also be established that the release of KP from the carrier faster and rather diffusion controlled when relatively small amount of electrostatic adsorbed surfactant molecules are present in the system. As the polymer-ionic surfactant interactions lead to changes in polymer structure the dissolution of the drug becomes slower, and the release turns to diffusion and erosion controlled way.

4. Conclusion

Since KP has some disadvantages as of low bioavailability and short half-life the formulation of controlled release dosage forms is needed. The results from both rheology and conductometric measurements verified the successful synthesis of two types of formulation by cross-linking of HyA or surface modification by CTAB. Turbidity, Zeta-potential and particle size analysis enabled the determination of optimal CTAB amount. The concentration-dependent structure of the HyA-based carrier was clearly confirmed by several rheological investigations. The release mechanism of KP from each formulation tested was evaluated in light of the first-order, Korsmeyer–Peppas and Weibull kinetic models. The release of KP

from the carrier is faster and rather diffusion controlled when relatively small amount of electrostatic adsorbed CTAB are present in the system. As the polymer-ionic surfactant interactions lead to changes in polymer structure the dissolution of drug becomes slower and the release turns to diffusion and erosion controlled way. However, the loading efficiency shows similar values (93-95%) but comparing the controlled drug release studies of our modified-HyA based systems with *e.g.* alginate-, gelatin- or acrylic polymer-based KP-containing systems we can conclude that after 4-6 h all of the amount of the encapsulated drug was dissolved from the above mentioned composites while in case of our systems (*e.g.* cl-HyA/100%) after 7 h only 70% but for CTAB/HyA 50% *ca.* only 40% of the KP content was dissolved. These results support the better applicability of cl-HyA NPs instead of the above mentioned other biocompatible carriers. We presented a potential applications of effective HyA biomaterial-based colloidal controlled drug release systems which contain hydrophobic NSAID KP molecule.

Acknowledgement

The research was supported by the National Research, Development and Innovation Office-NKFIH through the project K116323 and GINOP-2.3.2-15-2016-00060. This work was supported by the János Bolyai Research Fellowship of the Hungarian Academy of Sciences (E. Csapó). The authors thank the Richter Gedeon Nyrt. (Dr. Erika Forrai) for making the HyA available. The authors thank Prof. Botond Penke (University of Szeged, Department of Medical Chemistry) for his professional experience in this article.

References

Arida, A. I., & Al-Tabakha, M. M. (2007). Encapsulation of ketoprofen for controlled drug release. *European Journal of Pharmaceutics and Biopharmaceutics*, *66*(1), 48–54.

Barbucci, R., Consumi, M., & Magnani, A. (2002). Dependence of water uptake and morphology of hyaluronan- and alginate-based hydrogels on pH and degree of crosslinking. *Macromolecular Chemistry and Physics*, *203*(10–11), 1292–1300.

Benko, M., et al. (2015). Bovine serum albumin-sodium alkyl sulfates bioconjugates as drug delivery systems. *Colloids and Surfaces B: Biointerfaces*, *130*, 126–132.

Berkó, S., et al. (2013). Advantages of cross-linked versus linear hyaluronic acid for semisolid skin delivery systems. *European Polymer Journal*, *49*(9), 2511–2517.

Bodnár, M., et al. (2009). Preparation and characterization of cross-linked hyaluronan nanoparticles. *Colloid and Polymer Science*, *287*(8), 991–1000.

Choi, K. Y., et al. (2009). Self-assembled hyaluronic acid nanoparticles as a potential drug carrier for

411 cancer therapy: synthesis, characterization, and in vivo biodistribution. *Journal of Materials*
412 *Chemistry*, *19*(24), 4102-4107.
413 Costa, P., & Sousa Lobo, J. M. (2001, May 1). Modeling and comparison of dissolution profiles.
414 *European Journal of Pharmaceutical Sciences*. *13*(2), 123-133.
415 Csapó, E., et al. (2016). Thermodynamic and kinetic characterization of pH-dependent interactions
416 between bovine serum albumin and ibuprofen in 2D and 3D systems. *Colloids and Surfaces A:*
417 *Physicochemical and Engineering Aspects*, *504*, 471–478.
418 Danhier, F., Ansorena, E., Silva, J. M., Coco, R., Le Breton, A., & Préat, V. (2012). PLGA-based
419 nanoparticles: An overview of biomedical applications. *Journal of Controlled Release*, *161*(2),
420 505–522.
421 Deák, Á., Csapó, E., Juhász, Á., Dékány, I., & Janovák, L. (2018). Anti-ulcerant kynurenic acid
422 molecules intercalated Mg/Al-layered double hydroxide and its release study. *Applied Clay*
423 *Science*, *156*, 28–35.
424 Del Gaudio, P., Russo, P., Rosaria Lauro, M., Colombo, P., & Aquino, R. P. (2009). Encapsulation of
425 Ketoprofen and Ketoprofen Lysinate by Prilling for Controlled Drug Release. *AAPS*
426 *PharmSciTech*, *10*(4), 1178–1185.
427 Hashad, R. A., Ishak, R. A. H., Geneidi, A. S., & Mansour, S. (2017). Surface functionalization of
428 methotrexate-loaded chitosan nanoparticles with hyaluronic acid/human serum albumin:
429 Comparative characterization and in vitro cytotoxicity. *International Journal of Pharmaceutics*,
430 *522*(1–2), 128–136.
431 Iannitti, T., Bingöl, A. Ö., Rottigni, V., & Palmieri, B. (2013). A new highly viscoelastic hyaluronic
432 acid gel: Rheological properties, biocompatibility and clinical investigation in esthetic and
433 restorative surgery. *International Journal of Pharmaceutics*, *456*(2), 583–592.
434 Jiang, B.-P., et al (2015). Water-soluble hyaluronic acid–hybridized polyaniline nanoparticles for
435 effectively targeted photothermal therapy. *Journal of Materials Chemistry B*, *3*(18), 3767–3776.
436 Juhász, Á., Csapó, E., Ungor, D., Tóth, G. K., Vécsei, L., & Dékány, I. (2016). Kinetic and
437 Thermodynamic Evaluation of Kynurenic Acid Binding to GluR1 $_{270–300}$ Polypeptide by Surface
438 Plasmon Resonance Experiments. *The Journal of Physical Chemistry B*, *120*(32), 7844–7850.
439 Juhász, Á., Csapó, E., Vécsei, L., & Dékány, I. (2017). Modelling and characterization of the sorption
440 of kynurenic acid on protein surfaces. *Periodica Polytechnica Chemical Engineering*, *61*(1), 3–9.
441 Juhász, Á., Tabajdi, R., Dékány, I., & Csapó, E. (2017). Thermodynamic Characterization of
442 Temperature- and Composition-Dependent Mixed Micelle Formation in Aqueous Medium.
443 *Journal of Surfactants and Detergents*, *20*(6), 1291–1299.
444 Kargerová, A., & Pekař, M. (2014). High-Resolution Ultrasonic Spectroscopy Study of Interactions
445 between Hyaluronan and Cationic Surfactants. *Langmuir*, *30*(40), 11866–11872.
446 Király, Z., & Dekány, I. (2001). A thermometric titration study on the micelle formation of sodium
447 decyl sulfate in water. *Journal of Colloid and Interface Science*, *242*(1), 214–219.

448 Kumari, A., Yadav, S. K., & Yadav, S. C. (2010). Biodegradable polymeric nanoparticles based drug
449 delivery systems. *Colloids and Surfaces B: Biointerfaces*, *75*(1), 1–18.
450 Lee, G. Y., et al. (2015). Hyaluronic acid nanoparticles for active targeting atherosclerosis.
451 *Biomaterials*, *53*, 341–348.
452 Liang, J., & Krause, W. E. (2007). Rheology and lubricity of hyaluronic acid. *American Physical*
453 *Society, APS March Meeting, March 5-9, 2007, Abstract #N25.009*.
454 Maroda, M., et al. (2011). Preparation and investigation of a cross-linked hyaluronan nanoparticles
455 system. *Carbohydrate Polymers*, *83*(3), 1322–1329.
456 Mayol, L., et al. (2014). Amphiphilic hyaluronic acid derivatives toward the design of micelles for the
457 sustained delivery of hydrophobic drugs. *Carbohydrate Polymers*, *102*(1), 110–116.
458 Oueslati, N., et al. (2014). CTAB turbidimetric method for assaying hyaluronic acid in complex
459 environments and under cross-linked form. *Carbohydrate Polymers*, *112*, 102–108.
460 Padilla De Jesus, O. L., Ihre, H. R., Gagne, L., Frenchet, J. M. J., & Szoka, F. C. (2002). Polyester
461 dendritic systems for drug delivery applications: In vitro and in vivo evaluation. *Bioconjugate*
462 *Chemistry*, *13*(3), 453–461.
463 Palumbo, F. S., Pitarresi, G., Mandracchia, D., Tripodo, G., & Giammona, G. (2006). New graft
464 copolymers of hyaluronic acid and polylactic acid: Synthesis and characterization. *Carbohydrate*
465 *Polymers*, *66*(3), 379–385.
466 Pasqui, D., De Cagna, M., & Barbucci, R. (2012). Polysaccharide-based hydrogels: The key role of
467 water in affecting mechanical properties. *Polymers*, *4*(3), 1517–1534.
468 Peppas, N. A., & Merrill, E. W. (1977). Crosslinked poly(vinyl alcohol) hydrogels as swollen elastic
469 networks. *Journal of Applied Polymer Science*, *21*(7), 1763–1770.
470 Sauerová, P., et al. (2015). Hyaluronic acid as a modulator of the cytotoxic effects of cationic
471 surfactants. *Colloids and Surfaces A: Physicochemical and Engineering Aspects*, *483*, 155–161.
472 Vafaei, S. Y., et al. (2016). Self assembled hyaluronic acid nanoparticles as a potential carrier for
473 targeting the inflamed intestinal mucosa. *Carbohydrate Polymers*, *144*, 371–381.
474 Varga, N., Benko, M., Sebok, D., Bohus, G., Janovák, L., & Dékány, I. (2014). Mesoporous silica
475 core-shell composite functionalized with polyelectrolytes for drug delivery. *Microporous and*
476 *Mesoporous Materials*, *213*, 134–141.
477 Varga, N., Benko, M., Sebok, D., & Dékány, I. (2014). BSA/polyelectrolyte core-shell nanoparticles
478 for controlled release of encapsulated ibuprofen. *Colloids and Surfaces B: Biointerfaces*, *123*,
479 616–622.
480 Vučen, S. R., et al. (2013). Improved percutaneous delivery of ketoprofen using combined application
481 of nanocarriers and silicon microneedles. *Journal of Pharmacy and Pharmacology*, *65*(10),
482 1451–1462.
483 Wang, X., et al. (2017). Synthesis, characterization and liver targeting evaluation of self-assembled
484 hyaluronic acid nanoparticles functionalized with glycyrrhetinic acid. *European Journal of*

485 *Pharmaceutical Sciences*, *96*, 255–262.

Supplementary data

Click here to download Supplementary data: Revised Supporting Inf_Csapo_04_04.docx

Cross-linked and hydrophobized hyaluronic acid-based controlled drug release systems

Edit Csapó[a,b,*], Hajnalka Szokolai[b], Ádám Juhász[a,b], Norbert Varga[b], László Janovák[b], Imre Dékány[a,b]

Graphical abstract